

## Acoustic effects on nonlinear optical processes

Deckers, Steven; Van Steerteghem, Nick; Glorieux, Christ; Verbiest, Thierry; Van Der Veen, Monique A.

**DOI**

[10.1117/12.2236958](https://doi.org/10.1117/12.2236958)

**Publication date**

2016

**Document Version**

Final published version

**Published in**

Proceedings of SPIE

**Citation (APA)**

Deckers, S., Van Steerteghem, N., Glorieux, C., Verbiest, T., & Van Der Veen, M. A. (2016). Acoustic effects on nonlinear optical processes. In J. E. Haley, M. Eich, J. A. Schuller, & J.-M. Nunzi (Eds.), *Proceedings of SPIE : Light Manipulating Organic Materials and Devices III* (Vol. 9939). Article 99390F SPIE. <https://doi.org/10.1117/12.2236958>

**Important note**

To cite this publication, please use the final published version (if applicable).  
Please check the document version above.

**Copyright**

Other than for strictly personal use, it is not permitted to download, forward or distribute the text or part of it, without the consent of the author(s) and/or copyright holder(s), unless the work is under an open content license such as Creative Commons.

**Takedown policy**

Please contact us and provide details if you believe this document breaches copyrights.  
We will remove access to the work immediately and investigate your claim.

# PROCEEDINGS OF SPIE

[SPIDigitalLibrary.org/conference-proceedings-of-spie](https://spiedigitallibrary.org/conference-proceedings-of-spie)

## Acoustic effects on nonlinear optical processes

Steven Deckers, Nick Van Steerteghem, Christ Glorieux, Thierry Verbiest, Monique A. van der Veen

Steven Deckers, Nick Van Steerteghem, Christ Glorieux, Thierry Verbiest, Monique A. van der Veen, "Acoustic effects on nonlinear optical processes," Proc. SPIE 9939, Light Manipulating Organic Materials and Devices III, 99390F (23 September 2016); doi: 10.1117/12.2236958

**SPIE.**

Event: SPIE Organic Photonics + Electronics, 2016, San Diego, California, United States

# Acoustic effects on nonlinear optical processes

Steven Deckers\*<sup>a</sup>, Nick Van Steerteghem<sup>a</sup>, Christ Glorieux<sup>b</sup>, Thierry Verbiest<sup>a</sup>, Monique A. van der Veen<sup>c</sup>

<sup>a</sup>Molecular Electronics and Photonics, Department of Chemistry, KU Leuven, Celestijnenlaan 200D, B-3001 Heverlee, Belgium; <sup>b</sup>Laboratorium voor Akoestiek en Thermische Fysica, Departement Natuurkunde en Sterrenkunde, KU Leuven, Celestijnenlaan 200D, B-3001 Heverlee, Belgium; <sup>c</sup>Catalysis Engineering, Applied Sciences, Delft University of Technology, 2826 Delft, The Netherlands

## 1. ABSTRACT

We studied the effects of two types of ultrasonic waves, shear waves and longitudinal waves, using two nonlinear optical techniques, second-harmonic generation and hyper-Rayleigh scattering. Since shear waves hardly propagate in liquids, their influence on molecules at the interface between a surface and a liquid was studied using second-harmonic generation. Longitudinal waves propagate easily in solution, thus we used hyper-Rayleigh scattering to probe the ultrasonic effects on chromophores in solution. While we did not find shear waves to alter the second-harmonic generation from chromophores at the liquid/surface interface, the longitudinal waves caused effects comparable to our earlier observations. Longitudinal ultrasound caused a strong intensity modulation of the nonlinear optical signal according to a wave-pattern.

**Keywords:** nonlinear optics, ultrasound, second-harmonic generation, hyper-Rayleigh scattering

## 2. INTRODUCTION

Ultrasound irradiation has been fruitfully used in a variety of applications spanning medical imaging to synthetic chemistry.<sup>1-6</sup> In the field of medical imaging, modulation of fluorescence and enhancement of chemiluminescence by focused ultrasound is currently under study.<sup>7-9</sup> The goal is to overcome the detrimental effects of light scattering in biological tissue thereby enabling imaging deeper in the tissue.<sup>10-12</sup> Another method to enable imaging deeper in tissue is using nonlinear optical processes (such as multi-photon fluorescence (MPF) and second-harmonic generation (SHG)) instead of linear optical processes (such as fluorescence).<sup>13-15</sup> These nonlinear optical techniques take advantage of the so-called biological window in the near-infrared spectrum.<sup>13</sup> Using particular near-infrared wavelengths causes reduced photobleaching and photodamage in biological tissue compared with imaging techniques relying on linear optical processes such as fluorescence.<sup>13</sup> We have recently shown that ultrasound in the MHz-regime also causes fast and substantial signal intensity changes of hyper-Rayleigh scattering (HRS).<sup>16</sup> HRS is a second-order nonlinear optical technique in solution, it probes the first hyperpolarizability which is the ability of a molecule, often a chromophore, to nonlinearly scatter light.<sup>17</sup> We now direct our attention to ultrasonic shear waves on SHG from the interface between a surface and a liquid phase. An even-order nonlinear optical technique such as SHG is of great use in studying surfaces since SHG only arises if the local centrosymmetry is broken.<sup>18</sup> This occurs readily on surfaces which makes SHG highly sensitive to changes in this environment. Moreover, generating and detecting specific polarizations of second-harmonic light using laser light with a known polarization can be used to probe the orientation of adsorbed molecules.<sup>19-21</sup> Hence this technique could be of great use to probe chemical reactions at surfaces.<sup>22</sup> In case the first hyperpolarizability of the adsorbed molecule has one dominant contributing tensor element, such as  $\beta_{zzz}$  in the case of the studied chromophores<sup>21,23</sup>, this orientation angle can be determined from the SHG caused by two perpendicular polarizations of laser light.<sup>20</sup> The orientation of molecules has a great influence in chemical reactions.<sup>24-26</sup> Next to the temperature and activation energy the reacting molecules in a chemical reaction also need to be properly aligned in order to form the product. Hence manipulating the orientation of adsorbed molecules could be of great interest in heterogeneous catalysis.<sup>25</sup> In the chemical industry surfaces are often used to contain chemical catalysts or reactive groups such as acids.<sup>27</sup> Chemical reactors using those heterogeneous catalysts are usually controlled by manipulating the temperature,

flow rate, concentration and pressure of the used gasses, liquids or mixtures.<sup>24</sup> If one could reorient adsorbed molecules on demand, one could have a new approach to manipulate the reaction kinetics. How could these adsorbed molecules be reoriented near surfaces? Ultrasound irradiation could be an option since it has been used before to induce double refraction or birefringence in liquids of non-spherical molecules (or solutions of non-spherical particles).<sup>28–31</sup> Depending on the relaxation time of the molecules (or particles) different processes cause the ultrasonically induced birefringence. In case the particles under study are sufficiently small, the birefringence is caused by ultrasonically induced velocity gradients which exert a turning torque on the non-spherical molecules.<sup>32</sup> Currently this ultrasonically induced birefringence, and thus molecular reorientation, has only been studied in liquids using bulk longitudinal ultrasonic waves.<sup>28,33–40</sup> In this work we attempted to apply bulk shear waves at ultrasonic frequencies. Compared to longitudinal waves, that propagate through solids as well as through liquids, shear waves propagate through solids but hardly through liquids.<sup>41,42</sup> Because of this behavior we hypothesize that in liquids, in the direct vicinity of a substrate, these shear waves cause extremely strong velocity gradients. These velocity gradients would then in turn cause ultrasonically induced birefringence and thus reorientation of adsorbed non-spherical molecules. A lot of chromophores previously found in the literature regarding second-order nonlinear optics are in fact non-spherical, and could thus be sensitive to the ultrasonically induced velocity gradients.<sup>21,43–45</sup> We have examined the effects of shear waves at ultrasonic frequencies using two experimental situations. The first is the adsorption of a cationic chromophore on a substrate. The used chromophore has previously been used for in-situ observation of molecular adsorption by SHG.<sup>21</sup> The second experimental approach entails a chromophore covalently bound to the surface.<sup>22,46</sup> In accordance with our recent work we have also included two other examples of the ultrasound induced effect on HRS in the liquid phase.

### 3. EXPERIMENTAL SECTION

#### a. Cleaning of the glass substrates

As substrates, round slides made from common window glass and FGL455 colored filter glass slides (Thorlabs) were used. Both types of substrates were 25 mm in diameter, the substrates made from window glass were 1 mm thick while the colored glass filters were 2 mm thick. These colored glass optical filters were chosen in order to block possible second-harmonic light generated from the transducer to reach the detector. They do permit UV-Vis spectroscopy (in the vicinity of the wavelength of maximal absorbance of the chromophore) to detect the functionalization with the used chromophore, a dye resembling Disperse Red 1 with an added methyl group, azo-bond instead of the carbon-carbon double bond and the hydroxyl group replaced by an amine (see figure 1). Before silanization, the slides were cleaned by immersion in a Nochromix® cleaning solution for 3 h. The cleaning solution consisted of 7 g of Nochromix® powder with 100 mL distilled water and 100 mL sulfuric acid (Sigma Aldrich, ACS reagent grade, 95-97%). Afterwards the slides were cleaned with copious amounts of distilled water until the water waist had a neutral pH. Finally the slides were rinsed with methanol and dried for 30 minutes in an oven at 110 °C. To further clean the slides and render them hydrophilic they were then moved into an UV-ozone reactor for 1h.

#### b. Synthesis of chromophore modified slides using carbodiimide chemistry

Chromophore-modified substrates were made by the combination of click-chemistry and carbodiimide chemistry. The used chromophore and the resulting modified silane are shown in figure 1. Firstly, the substrates were silanized using a 1 V% solution of a carboxylic acid-terminated silane in toluene at room temperature for 1h. The carboxyl-terminated silane was synthesized using the method and reactor of Bloemen *et al.*<sup>47–49</sup> We adopted this method using 5 mol% 2,2-dimethoxy-2-phenylacetophenone (Sigma Aldrich, 99%) as an initiator and equal molar amounts of 3-mercaptopropyltrimethoxysilane (Sigma-Aldrich, 95%) and 10-undecenoic acid (Sigma-Aldrich, 96%) as reagents. Before adding the slides to the silanisation mixture, 4 drops of acetic acid (VWR, AnalaR NORMAPUR, 100%) were added to act as a catalyst. After the silanization step, the slides were washed by shaking 15 minutes in toluene (VWR, AnalaR NORMAPUR, 99.5%), 15 minutes in a 1:1 v/v toluene/methanol solution and finally 15 minutes in methanol. Then the slides dried in an oven for 1h at 110°C. After drying the slides were put in an aqueous solution containing 10 mM 1-ethyl-3-(3-dimethylaminopropyl)carbodiimide hydrochloride (EDC) (Thermo Fisher Scientific, 98%) and 40 mM N-hydroxysuccinimide (NHS) (Alfa Aesar, 98%) for 45 minutes. Then they were left to react overnight with a 0.3 mM solution of DR-NH<sub>2</sub> in THF (Sigma-Aldrich, BHT inhibited, 99.9%). Following the coupling of the chromophore the slides were washed with THF, MeOH and water for 15 minutes and dried in an oven for 15 minutes. The chromophore-modified substrate from window glass will be referred to as EN1 while the substrate consisting of the modified colored

filter glass will be referred to as EN2. The absorbance of the chromophore-modified substrates was measured using a Perkin Elmer lambda 900 UV-Vis spectrometer. For each type of chromophore-modified substrate, the absorbance was corrected for the absorbance of the unmodified substrate.

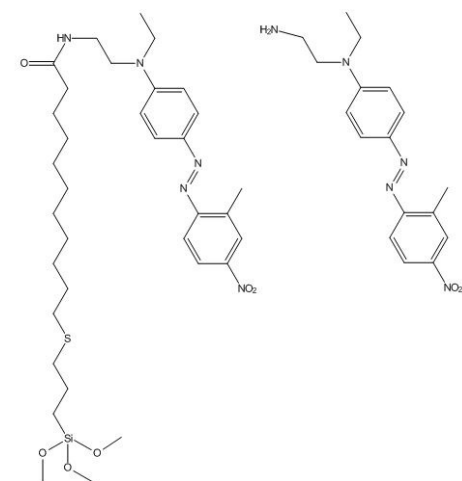


Figure 1. (left) The resulting chromophore-modified silane and (right) the individual chromophore used in the surface functionalization protocol. For clarity, the silane is drawn unbonded to the surface.

### c. Synthesis of slides Q using a topotactic quaternization protocol

This modification of the substrates was heavily based on the chromophoric self-assembly method by Ratner et al and Kakkar et al<sup>46,50</sup> and the subsequently developed topotactic quaternization method previously published by Lin *et al.*<sup>51,52</sup> The substrates were silanized using a 1V% solution of chloromethylphenyl triethoxy silane (ABCR, mixed m and p isomers) in toluene at room temperature for 1h. Before adding the slides to the silanisation mixture, 4 drops of acetic acid were added to act as a catalyst. After the silanization step, the slides were washed by shaking 15 minutes in toluene, 15 minutes in a 1:1 v/v toluene/methanol mixture and finally 15 minutes in methanol. Then the slides dried in an oven for 1h at 110°C. Then the slides were put in the center of a watch glass, a few drops of a 25mM precursor solution in 2-propanol (VWR, AnalaR NORMAPUR) were added on the center of the substrates. Then they were put in a vacuum oven for at least 3h at 120°C at a reduced pressure. The used chromophore precursor is 4-[4-(dimethylamino)styryl]pyridine (Sigma-Aldrich, 95%). The presence of the synthesis product, a cationic chromophore, can be readily checked by UV-Vis spectroscopy by the disappearance of the precursor absorbance peak and rise of a new absorbance peak at a higher wavelength.<sup>50</sup> After the chromophore coupling, the substrates were washed with 2-propanol and twice with MeOH for 15 minutes. The sample Q1 used for the SHG-experiments consisted of a chromophore-modified colored filter glass. The absorbance of the chromophore-modified substrates was measured using a Perkin Elmer lambda 900 UV-Vis spectrometer. For each type of chromophore-modified substrate, the absorbance was corrected for the absorbance of the unmodified substrate.

### d. Second-harmonic generation: adsorption experiments

The used substrates were FGL455 colored glass filters from Thorlabs. After the cleaning step they were mounted in a homemade measurement cell. Adsorption experiments were conducted using 20  $\mu$ M solutions of trans-4-[4-(dimethylamino)styryl]-1-methylpyridinium iodide (Sigma-Aldrich, 98%) in 2-propanol and 1-hexanol (Sigma-Aldrich, 98%). In the remainder of this text we will refer to trans-4-[4-(dimethylamino)styryl]-1-methylpyridinium iodide as DAMPI. An ultrasonic transducer, a ceramic shear plate (70-5015, American Piezo, 850 material, Navy II, 1MHz) or a shear transducer (Olympus, V155-SM UT, 5MHz) is firmly clamped to the mounted substrate by the construction of the measurement cell. To ensure a good coupling between the transducer and the substrate, a thin layer of shear gel (Olympus, SWC, normal incidence shear gel) was added to the substrate before clamping the transducer. A Tektronix 2101 function generator excited the transducers at various frequencies at a voltage amplitude of 10 Vpp.

#### **e. Second-harmonic generation: functionalized substrates**

The chromophore-modified substrates are mounted in a homebuilt measurement cell. An ultrasonic transducer, a 1 MHz ceramic shear plate or a 5 MHz shear transducer is firmly clamped to the mounted substrate by the construction of the measurement cell. To ensure a good coupling between the transducer and the substrate, a thin layer of shear gel was added to the substrate before clamping the transducer. A Tektronix 2101 function generator excited the transducers at various frequencies at a voltage amplitude of 10 Vpp.

#### **f. Second-harmonic generation setup**

The second-harmonic signal was generated by a femtosecond laser operating at 800 nm. The average output power of the laser is 2.3 W but was lowered significantly (average power 200 mW) to prevent laser-induced damage to the samples under study. The setup is shown in figure 2. The femtosecond laser (a) is driven by a solid state laser (b, Spectra Physics, Millennia Pro) operating at 11.5 W. The second-harmonic light was detected in a reflection geometry with the angle between the laser and sample normal (c) fixed at 45 degrees. A combination of a half wave plate (d) and a Glan-Laser calcite polarizer (e, Thorlabs GL10-B) is used to control the average power intensity of the fundamental laser beam. The polarizer is polarized parallel to the optical table, thus operates in P-polarization. Another half wave plate (f) is mounted in a computer controlled rotation stage in order to change the polarization of the fundamental laser light prior to being focused on the sample. The fundamental laser light is chopped by a mechanical chopper (g) operating at 770 Hz. This frequency is also directed into the reference input of a lock-in amplifier (h, Stanford Research SR830). In the beam path before the laser reaches the sample, a filter is inserted to remove second-harmonic light originating from the used optics or laser cavity (i). A manual diaphragm (j) is used to select the reflections from the sample in the measurement cell (k). Both the second-harmonic light and the fundamental laser light reflected from the sample are collimated using a planoconvex lens (l). A 1 mm thick BG39 filter (m) removes the fundamental laser light from the second-harmonic light. The second-harmonic light then passes through a second Glan-Laser calcite polarizer (n, Thorlabs GL10-A) aligned according to P-polarization. Then a lens (o) focuses the second-harmonic light on a photomultiplier tube (p, Hamamatsu, 9800) which is adapted with an interference filter (q) to select the proper wavelength.

The output power of the laser gradually declined over time. We have corrected for this inconvenience by insertion of a reference branch as is shown in figure 2. This branch measures SHG from a piece of Y-quartz (r) that is irradiated with 5 mW of the fundamental 800 nm laser light. The detector used in this reference branch (s) is the same type as the measurement branch. In both the reference and measurement line a BG39 filter and an band-pass filter with its transmitting wavelength interval centered around 400 nm were used to discriminate the second-harmonic light from the laser light.

In figure 2, electrical connections are shown by dashed lines, the SHG signal by blue lines and the fundamental laser by red lines.

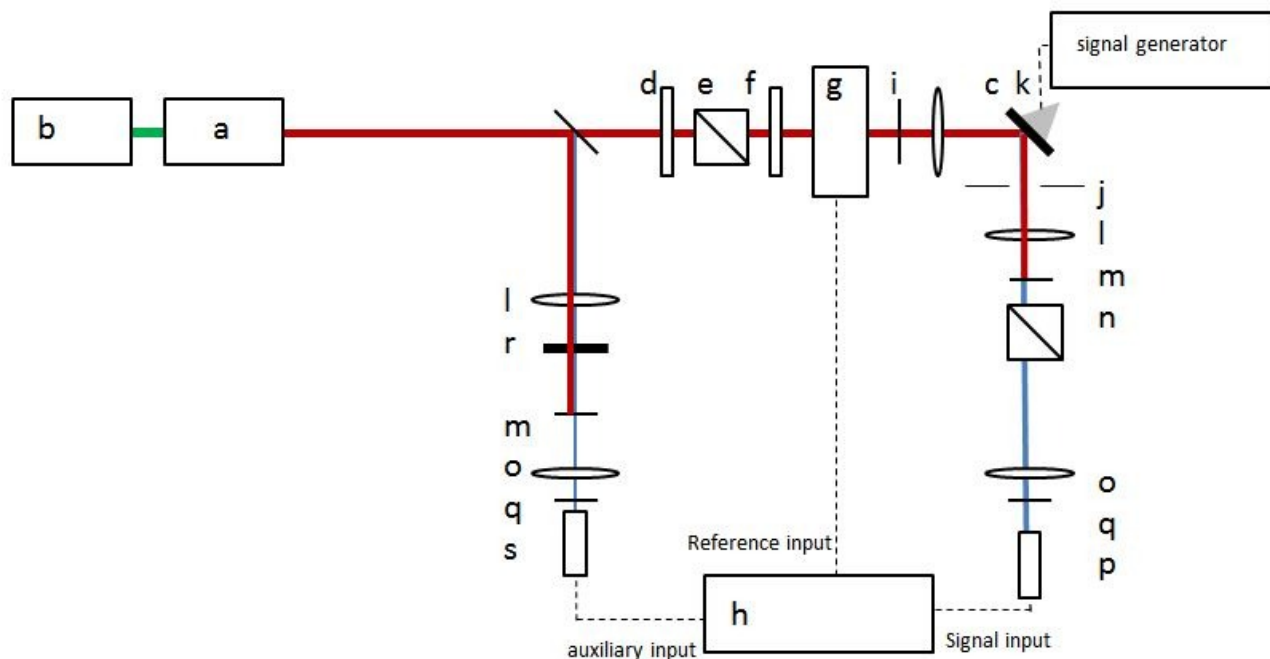


Figure 2. The used SHG setup, operating at 800 nm (red line), the SHG signal is represented by the blue line, the electrical connections are represented by the dashed line.

#### g. Hyper-Rayleigh scattering setup

The used hyper-Rayleigh setup was a traditional setup using lock-in detection with a rotating chopper.<sup>53</sup> We know from our previous work which was recently submitted elsewhere,<sup>16</sup> that both HRS and MPF behave similarly under ultrasound irradiation. Therefore we did not attempt to discriminate between HRS and MPF using the high frequency demodulation technique. The sample used was a solution of DAMPI in chloroform. Just as is the case with Disperse Red 1, which was used in our previous publication, DAMPI is a rodlike chromophore with a first hyperpolarizability dominated by the  $\beta_{zzz}$  tensor element along the Z-axis, the molecular axis. We have used one transducer-modified cuvette, the same as in our previous publication. This cuvette is a standard H€ellma optical glass cuvette with an optical path length of 2 mm. The transducer, a piezoceramic element (American Piezo, 850 material, Navy II) with a thickness of 2 mm was attached to this cuvette using conducting glue (Holland Shielding Systems).

## 4. RESULTS AND DISCUSSION

### a. Synthesis and characterization of covalently attached chromophores

After being dried, the absorbance of the chromophore-modified substrates was determined. From figure 3, it is clear that both the common window glass as the FGL455 filter show a comparable absorbance. The chromophore has an intense absorbance peak centered around 500 nm. The Q1 sample only showed a weak absorbance peak. The unstable behavior of the absorbance at wavelengths lower than 470 nm arise from a mismatch between the colored glass filter used to take the baseline and the chromophore-modified colored glass filter. After several days after its synthesis the second-harmonic signal from the Q1 sample disappeared while the second-harmonic signal from EN1 and EN2 sample remained nearly unchanged. Also the method using the NHS/EDC-protocol proved to yield more consistent results compared to the topotactic method.

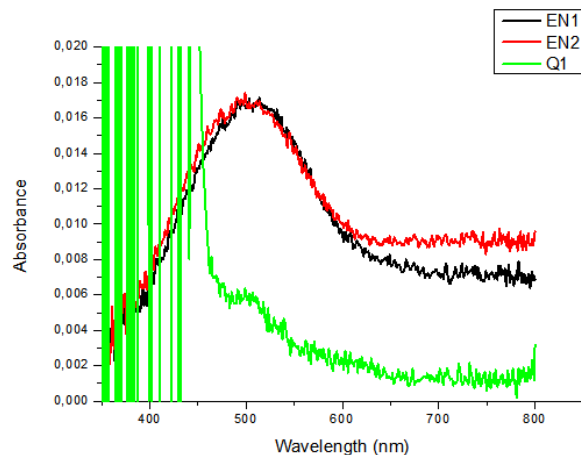


Figure 3: Absorbance spectra of chromophore-modified substrates. A common window glass substrate with disperse dye DR (black) and the chromophore-modified colored filter glass (red) showed a much higher absorbance than the substrate modified using a topotactic quaternization reaction resulting in a cationic chromophore (green).

#### b. Acoustic effects on Second-Harmonic Generation from adsorbed chromophores

Cleaned substrates were installed in a homemade measurement cell. Then the chromophore solution is added using a syringe. Homemade software was used to change the applied ultrasonic frequency while for each frequency the half wave plate was rotated to P- and S-polarization. For each combination of applied ultrasonic frequency and polarization angle the P-polarized second-harmonic signal from the sample was obtained. These signals were corrected for changes in laser intensity (and time dependent changes in pulse width) by taking the ratio with the intensity of a reference sample. Then the depolarization ratio, the ratio of the SHG intensity generated by P-polarized laser light with the SHG generated by the S-polarized laser light, can be used to determine the orientation angle of adsorbed molecules.<sup>54</sup> The ultrasonic frequency was varied in a wide range around the resonance frequencies of the Olympus transducer at 4.9 MHz and 7 MHz. These data are plotted in figure 4. It is clear that for the studied frequency range, and for solutions in two solvents with a different viscosity, no ultrasound-induced effects are present on the SHG signal from adsorbed DAMPI. We want to make clear that, while the SHG intensity by the S-polarized laser light was clearly measurable while the SHG from the P-polarized signal was much lower in intensity. Therefore we chose to measure the possible ultrasonic effects of the 1 MHz shear plate on the SHG using a fixed polarization of the fundamental laser light. The laser light was polarized at 22.5°, an angle centered between S- and P-polarization. This approach probes simultaneously changes in P-polarized SHG by P- or S-polarized incident laser light. The applied ultrasonic frequency was again varied in a wide range around the resonance frequency of the transducer. The results are plotted in figure 5. No effect of the applied ultrasonic frequencies was observed on the SHG signal. This implies again no molecular reorientation occurs upon excitation of ultrasonic shear waves. We have seen a time-dependency of the SHG-signal which we attribute to laser-induced desorption or an irreversible photobleaching effect.



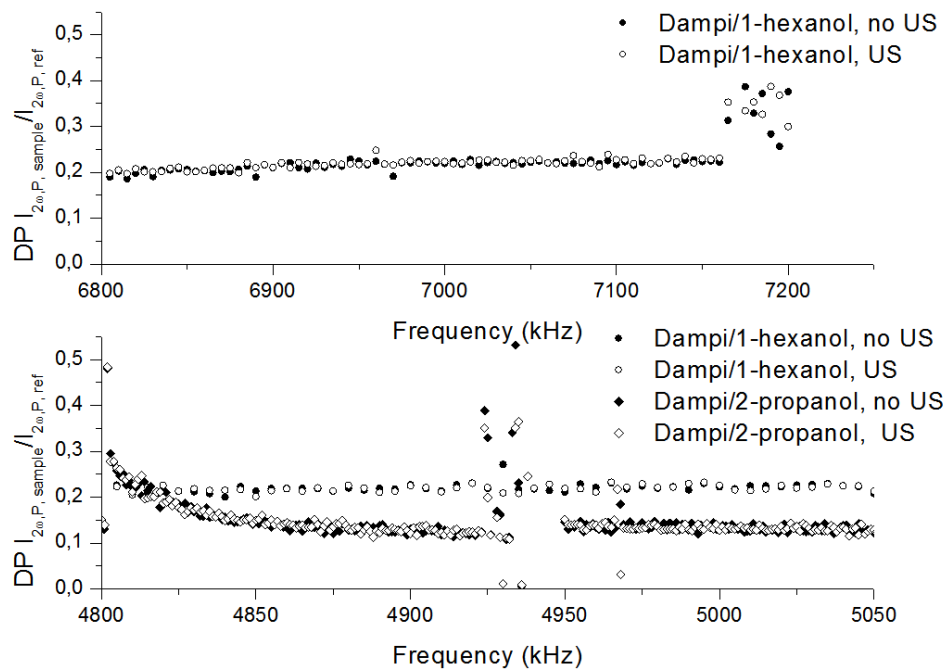


Figure 4. The depolarization ratio of adsorbed DAMPI from a solution in 1-hexanol and 2-propanol upon excitation of shear waves at ultrasonic frequencies. Two frequency ranges were chosen, one around the resonance frequency of the unmounted transducer(bottom) and one around the impedance minimum of the transducer clamped to the substrate(top).

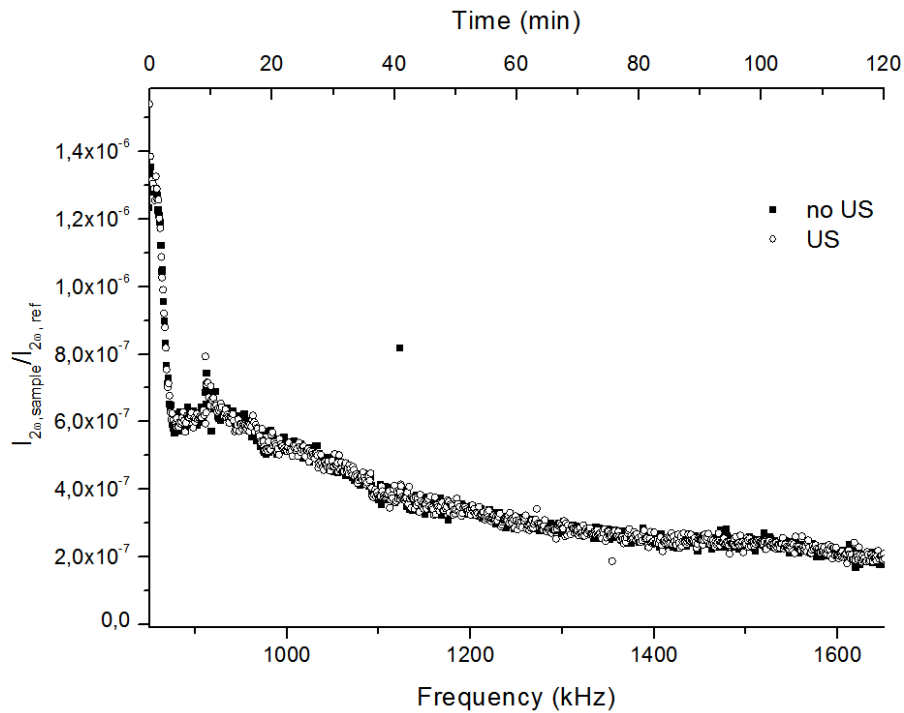


Figure 5: The second-harmonic intensity of DAMPI adsorbed on the surface from a solution in 1-hexanol upon application of shear waves. The shear waves were excited by a clamped shear plate with a resonance frequency around 1 MHz. The detected second-harmonic light is polarized according to the P-polarization while the laser beam is polarized at an angle of 22.5° which is the angle centered between S-and P-polarization.

### c. Acoustic effects on Second-harmonic Generation from chromophore-modified substrates

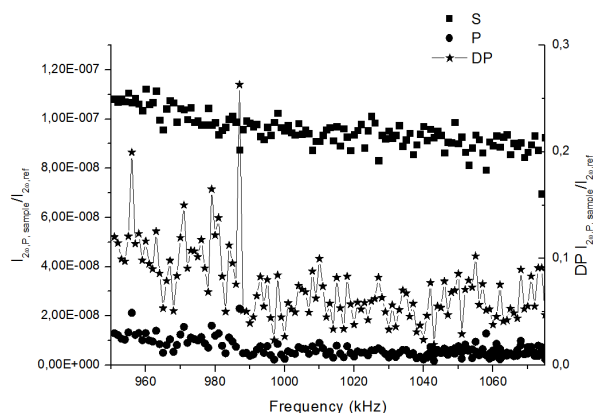


Figure 6. P-polarized SHG from a cationic chromophore covalently coupled to the surface. For two polarizations, P- and S-polarization, of the incoming laser light the applied shear frequency was changed from 900 kHz to 1080 kHz in 1 kHz steps.

Since the adsorption experiments did not show any frequency-dependent effects in the orientation angle of the adsorbed molecules or their SHG intensity, we chose to use chemically-modified substrates instead. These chemically-modified substrates were synthesized using two methods that were already used in literature. The first one is a simple quaternization reaction between a chromophore precursor with a surface-bound halogen-functionalized silane.<sup>46,55-59</sup> The second method is a coupling reaction between an amine and a carboxylic acid using carbodiimide chemistry. In this method the silane contains an 11 carbon long spacer, hence the chromophore is supposedly much more mobile than the one coupled using the first method. We chose to use the 1 MHz shear plate to excite the shear waves. Firstly we determined the P-polarized SHG from the Q1 sample by S- and P-polarized laser light while applying shear waves at different ultrasonic frequencies. The solvent was 1-hexanol. The shear frequency was increased from 950 kHz to 1080 kHz in 1 kHz steps. The results are plotted in figure 6. Clearly just as was the case with physically adsorbed DAMPI the SHG from S-polarized laser light overwhelmed the SHG from P-polarized laser light. During the frequency scan, along the x-axis (which can thus also be interpreted as a time axis), the SHG from both laser polarizations declined over time. This translates to a decline in the depolarization ratio, inferring an orientation change, but this is probably a bleaching effect.

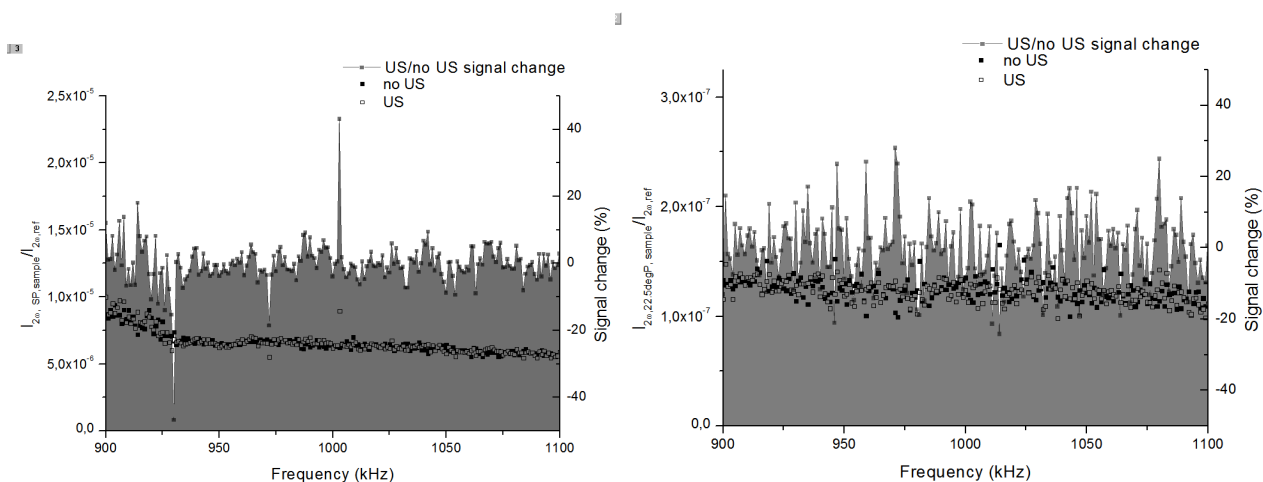


Figure 7. The P-polarized SHG from covalently bound chromophores EN under MHz shear wave irradiation. The SHG was excited using S-polarized laser light. (left) In order to probe changes in SHG caused by shear waves and either S- or P-polarized laser light the half wave plate was to 22.5° (right). The frequency of the shear waves was scanned from 900 kHz to 1100 kHz in 1 kHz steps. The solvent was 1-hexanol.

We then probed the P-polarized SHG from the EN sample (see figure 7). The solvent was again 1-hexanol. Because the intensity of the SHG from P-polarized laser light was hardly visible from the background we chose to focus our attention to the SHG from S-polarized laser light. This however only probes SHG-contributions from tensor components oriented flat on the surface. In case the shear waves lower the alignment angle a peak in the SHG would arise at a particular frequency. In figure 7 we see that the SHG signals from S-polarized laser light with and without shear waves are hardly discernible from each other. Again the SHG intensity declines during the first part of the measurement which is attributed to an irreversible bleaching effect. We also plotted the percentage change of the SHG signal upon shear wave irradiation. These changes are largely confined between signal increases and decreases of 10% and show no clear dependency on the applied ultrasonic frequency. We then followed the approach we previously used with the quaternized sample Q1. The polarization angle of the laser light was fixed at  $22.5^\circ$  in order to simultaneously probe the SHG intensity from S-and P-polarized laser light. As can be seen in figure 7, the SHG intensity does not change upon shear wave irradiation.

#### d. Results acoustic effects on hyper-Rayleigh scattering

In our previous paper we studied the effects of density waves at ultrasonic frequencies on two nonlinear optical processes that occur in solution, hyper-Rayleigh scattering (HRS) and multiphoton fluorescence (MPF).<sup>16</sup> In order to make the distinction between both nonlinear optical effects we used an experimental setup using a spectrograph and electron multiplying CCD camera.<sup>16</sup> Because in the past a lot of work regarding HRS was conducted using techniques relying on lock-in amplification we now repeated these experiments in a classical HRS setup using another chromophore, DAMPI.<sup>60,61</sup> We used the setup with frequency demodulation at 80 MHz.<sup>62,63</sup> The used solvent is chloroform to retain the resonance frequency of the measurement cell at 990 kHz. We did not attempt to differ between MPF and HRS. Since we attributed the ultrasonic effects to originate from the ultrasonically induced density gradients we expect the same behavior to occur using a different chromophore and setup. Firstly we studied the voltage dependency of the ultrasound-modulated nonlinear optical response. The result is shown in figure 8a. In accordance with our previous results, a linear relationship is observed between the nonlinear optical signal increase and the voltage amplitude applied on the transducer.<sup>16</sup> We have also probed the ultrasonic effects on the nonlinear optical intensity at different positions in the measurement cell. Over a distance of 1.1 mm we took a series of measurements in 5  $\mu\text{m}$  steps. This is shown in figure 8b. As expected the ultrasound induced intensity increased according to the a standing wave pattern.<sup>16</sup> The ultrasound was applied according to a sinusoidal pattern hence the NLO signal varies accordingly to the absolute value of the applied waveform. This infers that the conclusions from our previous publication can be applied to other anisotropically shaped chromophores with a dominating axial hyperpolarizability  $\beta_{zzz}$ .

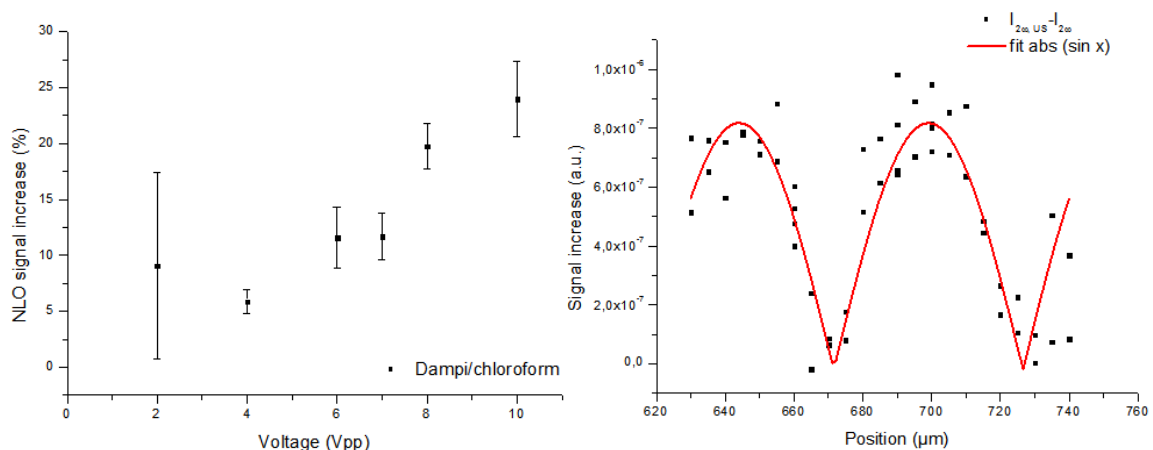


Figure 8. (left) The voltage dependence of the NLO signal increase. (right) The induced intensity modulation follows a standing wave pattern.

## 5. CONCLUSION

We have studied the effects of shear waves at ultrasonic frequencies on non-spherical chromophores near substrates and confirmed the previously found effects of longitudinal ultrasound on the nonlinear optical properties of non-spherical chromophores in solution.<sup>16</sup> We have used two different ultrasonic transducers operating at two frequency regions to excite the shear waves and a large ultrasonic frequency range was scanned. Both for adsorbed and covalently attached chromophores no change in SHG-signal was observed with ultrasonic shear wave irradiation. Following adsorption or immersion in a solvent of a chromophore-modified substrate, the dominant contribution to the second-harmonic signal indicated the chromophores to reside in both cases flat to the surface. In contrast to the absence of ultrasonically-induced effects on the nonlinear optical properties of chromophores near surfaces, an ultrasonically-induced effect on the hyper-Rayleigh scattering of two chromophores in solution was shown. We have recently found this effect to occur with a Disperse Red 1 solution in chloroform and have confirmed its presence with another non-spherical chromophore, trans-4-[4-(dimethylamino)styryl]-1-methylpyridinium iodide using a different experimental setup.

## 6. ACKNOWLEDGEMENT

M.A.v.d.V. and N.V.S acknowledge FWO-Vlaanderen for their personal fellowships. C.G acknowledges FWO-Vlaanderen for financial support (research project FWO research project G.0360.09). The authors acknowledge Dirk Devos for his valuable contribution. We are also grateful to the Onderzoeksfonds KU Leuven/Research Fund KU Leuven for a CREA grant. We are also grateful to the divisions Molecular Design and Synthesis and Polymer Chemistry and Materials of KU Leuven for the delivery of specific chemicals like the amino-terminated chromophore.

### References

- [1] Shung, K. K., Cannata, J. M., Zhou, Q. F., "Piezoelectric materials for high frequency medical imaging applications: A review," *J. Electroceramics* **19**(1), 141–147 (2007).
- [2] James, J., Mrukeshan, V. M., Woh, L. S., "Integrated photoacoustic , ultrasound and fluorescence platform for diagnostic medical imaging-proof of concept study with a tissue mimicking phantom," *Biomed. Opt. Express* **5**(7), 2135–2144 (2014).
- [3] Jain, L., Singh, P., "A Historical and Qualitative Analysis of Different Medical Imaging Techniques," *Int. J. Comput. Appl.* **107**(15), 4–8 (2014).
- [4] Cui, C., Zhu, C., Du, X.-J., Wang, Z.-P., Li, Z.-M., Zhao, W.-G., "Ultrasound-promoted sterically congested Passerini reactions under solvent-free conditions," *Green Chem.* **14**(11), 3157 (2012).
- [5] Ruecroft, G., Hipkiss, D., Ly, T., Maxted, N., Cains, P. W., "Sonocrystallization: The Use of Ultrasound for Improved Industrial Crystallization," *Org. Process Res. Dev.* **9**(6), 923–932 (2005).
- [6] Cravotto, G., Cintas, P., "Power ultrasound in organic synthesis: moving cavitation chemistry from academia to innovative and large-scale applications.," *Chem. Soc. Rev.* **35**(2), 180–196 (2006).
- [7] Zhou, Y., Yao, J., Wang, L. V., "Tutorial on photoacoustic tomography," *J. Biomed. Opt.* **21**(6), 061007 (2016).
- [8] Bingbing Cheng., Ming-Yuan Wei., Yuan Liu., Pitta, H., Zhiwei Xie., Yi Hong., Nguyen, K. T., Baohong Yuan., "Development of Ultrasound-Switchable Fluorescence Imaging Contrast Agents Based on Thermosensitive Polymers and Nanoparticles," *IEEE J. Sel. Top. Quantum Electron.* **20**(3), 67–80 (2014).
- [9] Benchimol, M. J., Hsu, M. J., Schutt, C. E., Hall, D. J., Mattrey, R. F., Esener, S. C.,

- “Phospholipid/Carbocyanine Dye-Shelled Microbubbles as Ultrasound-Modulated Fluorescent Contrast Agents,” *Soft Matter* **9**(8), 2384–2388 (2013).
- [10] Kobayashi, M., Kikuchi, N., Sato, A., “Optical tomography of fluorophores in dense scattering media based on ultrasound-enhanced chemiluminescence,” *Appl. Phys. Lett.* **106**(2), 021103 (2015).
- [11] Kobayashi, M., Mizumoto, T., Duc, T. Q., Takeda, M., “Fluorescence Tomography of Biological Tissue Based on Ultrasound Tagging Technique,” *Proc. SPIE 6633, Biophotonics 2007 Opt. Life Sci.* **6633**, J. Popp and G. von Bally, Eds., 663306–663306 – 5 (2007).
- [12] Kobayashi, M., Mizumoto, T., Shibuya, Y., Enomoto, M., Takeda, M., “Fluorescence tomography in turbid media based on acousto-optic modulation imaging,” *Appl. Phys. Lett.* **89**(18), 1–4 (2006).
- [13] Masters, B. R., So, P. T. C., *Handbook of Biomedical Nonlinear Optical Microscopy*, Oxford University Press, Inc, New York (2008).
- [14] De Meulenaere, E., Nguyen Bich, N., de Wergifosse, M., Van Hecke, K., Van Meervelt, L., Vanderleyden, J., Champagne, B., Clays, K., “Improving the second-order nonlinear optical response of fluorescent proteins: the symmetry argument,” *J. Am. Chem. Soc.* **135**(10), 4061–4069 (2013).
- [15] De Meulenaere, E., Chen, W.-Q., Van Cleuvenbergen, S., Zheng, M.-L., Psilodimitrakopoulos, S., Paesen, R., Taymans, J.-M., Ameloot, M., Vanderleyden, J., et al., “Molecular engineering of chromophores for combined second-harmonic and two-photon fluorescence in cellular imaging,” *Chem. Sci.* **3**(4), 984 (2012).
- [16] Deckers, S., Van Steerteghem, N., Glorieux, C., Verbiest, T., van der Veen, M. A., “Intense Signal Modulation of Nonlinear Optical Scattering and Multiphoton Fluorescence by Ultrasound Irradiation,” *Recent. Submitt. to Phys. Chem. C* (2016).
- [17] Clays, K., Persoons, A., “Hyper-Rayleigh Scattering in Solution,” *Phys. Rev. Lett.* **66**(23), 2980–2983 (1991).
- [18] Boyd, R., *Nonlinear Optics*, San Diego: Academic Press (1992).
- [19] Corn, R. M., Higgins, D. a., “Optical second harmonic generation as a probe of surface chemistry,” *Chem. Rev.* **94**(1), 107–125 (1994).
- [20] Heinz, T., Tom, H., Shen, Y., “Determination of molecular orientation of monolayer adsorbates by optical second-harmonic generation,” *Phys. Rev. A* **28**(3), 1883–1885 (1983).
- [21] van der Veen, M. a., Valev, V. K., Verbiest, T., De Vos, D. E., “In situ orientation-sensitive observation of molecular adsorption on a liquid/zeolite interface by second-harmonic generation,” *Langmuir* **25**(8), 4256–4261 (2009).
- [22] Roscoe, S. B., Yitzchaik, S., Kakkar, A. K., Marks, T. J., Xu, Z., Zhang, T., Lin, W., Wong, G. K., “Self-Assembled Chromophoric NLO-Active Structures. Second-Harmonic Generation and X-ray Photoelectron Spectroscopic Studies of Nucleophilic Substitution and Ion Exchange Processes on Benzyl Halide-Functionalized Surfaces,” *Langmuir* **12**(22), 5338–5349 (1996).
- [23] Campo, J., Desmet, F., Wenseleers, W., Goovaerts, E., “Highly sensitive setup for tunable wavelength hyper-Rayleigh scattering with parallel detection and calibration data for various solvents,” *Opt. Express* **17**(6), 4587–4604 (2009).
- [24] Özkan, L., Backx, T., Van Gerven, T., Stankiewicz, a. I., “Towards Perfect Reactors: Gaining full control of chemical transformations at molecular level,” *Chem. Eng. Process. Process Intensif.* **51**, 109–116, Elsevier B.V. (2012).

- [25] Hou, H., "The Stereodynamics of a Gas-Surface Reaction," *Science* (80-. ). **277**(5322), 80–82 (1997).
- [26] Loesch, H., "Orientation and Alignment in Reactive Beam Collisions: Recent Progress," *Annu. Rev. Phys. Chem.* **46**(1), 555–594 (1995).
- [27] Sheldon, R. ., Downing, R. ., "Heterogeneous catalytic transformations for environmentally friendly production," *Appl. Catal. A Gen.* **189**(2), 163–183 (1999).
- [28] Hilyard, N. C., Jerrard, H. G., "Theories of Birefringence Induced in Liquids by Ultrasonic Waves," *J. Appl. Phys.* **33**(12), 3470 (1962).
- [29] Lipeles, R., Kivelson, D., "Experimental studies of acoustically induced birefringence," *J. Chem. Phys.* **72**(11), 6199–6208 (1980).
- [30] Yasuda, K., Matsuoka, T., Koda, S., Nomura, H., "Frequency Dependence of Ultrasonically Induced Birefringence of Rodlike Particles," *J. Phys. Chem.* **100**(14), 5892–5897 (1996).
- [31] Nomura, H., Matsuoka, T., Koda, S., "Ultrasonically induced birefringence in polymer solutions," *Pure Appl. Chem.* **76**(1), 97–104 (2004).
- [32] Nomura, H., Ando, S., Matsuoka, T., Koda, S., "Effect of chain structure and molecular weight on ultrasonically induced birefringence in polymer solutions," *J. Mol. Liq.* **103-104**, 111–119 (2003).
- [33] Jerrard, G., "Birefringence induced in liquids and solutions by ultrasonic waves," *Ultrasonics* **April-June**, 74–81 (1964).
- [34] Martinoty, P., Bader, M., Martinoty, P., Measurement, M. B., "Measurement of the birefringence induced in liquids by ultrasonic waves: application to the study of the isotropic phase of PAA near the transition point," *J. Phys.* **42**(8), 1097–1102 (1981).
- [35] Bader, M., Martinoty, P., "Birefringence Induced by Ultrasonic Waves in the Isotropic Phase of PCB," *Mol. Cryst. Liq. Cryst.* **76**(3-4), 269–277 (1981).
- [36] Ou-Yang, H., MacPhail, R., Kivelson, D., "Nonlinear ultrasonically induced birefringence in gold sols: Frequency-dependent diffusion.," *Phys. Rev. A* **33**(1), 611–619 (1986).
- [37] Koda, S., Koyama, T., Enomoto, Y., Nomura, H., "Study on Orientational Motion of Liquid Crystals by Acoustically Induced Birefringence," *12TH SYMP Ultrason. Electron.* **31**, 51–53, JAPAN J APPLIED PHYSICS, DAINI TOYOKAIJI BLDG 24-8 SHINBASHI 4-CHOME, MINATO-KU TOKYO 105, JAPAN, TOKYO, JAPAN (1992).
- [38] Matsuoka, T., Yasuda, K., Koda, S., Nomura, H., "On the frequency dependence of ultrasonically induced birefringence in isotropic phase of liquid crystal: 5CB (p-n-pentyl p[<sup>sup</sup>]-cyanobiphenyl)," *J. Chem. Phys.* **111**(4), 1580 (1999).
- [39] Matsuoka, T., Yasuda, K., Yamamoto, K., Koda, S., Nomura, H., "Dynamics of ultrasonically induced birefringence of in rod-like colloidal solutions.," *Colloids Surf. B. Biointerfaces* **56**(1-2), 72–79 (2007).
- [40] Nomura, H., Ando, S., Matsuoka, T., Koda, S., "Relationship between segmental anisotropy in polarizability and stationary ultrasonically induced birefringence in polymer solutions," *J. Mol. Liq.* **110**(1-3), 57–62 (2004).
- [41] Kaspar, M., Stadler, H., Weiss, T., Ziegler, C., "Thickness shear mode resonators ('mass-sensitive devices') in bioanalysis," *Fresenius. J. Anal. Chem.* **366**(6-7), 602–610 (2000).
- [42] Shutilov, V. A., *Fundamental physics of ultrasound* (1988).
- [43] Cheng, L. T., Tam, W., Stevenson, S. H., Meredith, G. R., Rikken, G., Marder, S. R., "Experimental investigations of organic molecular nonlinear optical polarizabilities. 1. Methods and results on benzene and stilbene derivatives," *J. Phys. Chem.* **95**(26), 10631–

- 10643 (1991).
- [44] Shoute, L. C. T., Woo, H. Y., Vak, D., Bazan, G. C., Myers Kelley, A., “Solvent effects on resonant first hyperpolarizabilities and Raman and hyper-Raman spectra of DANS and a water-soluble analog,” *J. Chem. Phys.* **125**(5), 054506 (2006).
- [45] Kajikawa, K., Yoshida, I., Seki, K., Ouchi, Y., “Orientational structure in hemicyanine self-assembled films studied by absorption spectroscopy and optical second-harmonic generation,” *Chem. Phys. Lett.* **308**(3-4), 310–316 (1999).
- [46] Kakkar, A. K., Yitzchaik, S., Roscoe, S. B., Marks, T. J., Lin, W., Wong, G. K., “Self-assembled chromophoric thin film NLO materials. Effect of coupling agent surface functionalization and ion exchange processes on second harmonic generation characteristics,” *Thin Solid Films* **242**(1-2), 142–145 (1994).
- [47] Bloemen, M., Denis, C., Peeters, M., De Meester, L., Gils, A., Geukens, N., Verbiest, T., “Antibody-modified iron oxide nanoparticles for efficient magnetic isolation and flow cytometric determination of *L. pneumophila*,” *Microchim. Acta* **182**(7-8), 1439–1446 (2015).
- [48] Lowe, A. B., “Thiol-ene ‘click’ reactions and recent applications in polymer and materials synthesis,” *Polym. Chem.* **1**(1), 17 (2010).
- [49] Hoyle, C. E., Lee, T. Y., Roper, T., “Thiol-enes: Chemistry of the past with promise for the future,” *J. Polym. Sci. Part A Polym. Chem.* **42**(21), 5301–5338 (2004).
- [50] Li, D., Ratner, M. A., Marks, T. J., Zhang, C., Yang, J., Wong, G. K., “Chromophoric Self-Assembled Multilayers. Organic Superlattice Approaches to Thin-Film Nonlinear Optical Materials,” *J. Am. Chem. Soc.* **112**(c), 7389–7390 (1990).
- [51] Lin, W., Lin, W., Wong, G. K., Marks, T. J., “Supramolecular Approaches to Second-Order Nonlinear Optical Materials. Self-Assembly and Microstructural Characterization of Intrinsically Acentric [(Aminophenyl)azo]pyridinium Superlattices,” *J. Am. Chem. Soc.* **118**(34), 8034–8042 (1996).
- [52] Marks, T. J., Yitzchaik, S., “Chromophoric Self-Assembled Superlattices,” *Acc. Chem. Res.* **29**(4), 197–202 (1996).
- [53] Deckers, S., Vandendriessche, S., Cornelis, D., Monnaie, F., Koeckelberghs, G., Asselberghs, I., Verbiest, T., van der Veen, M. A., “Poly(3-alkylthiophene)s show unexpected second-order nonlinear optical response,” *Chem. Commun. (Camb)*. **50**(21), 2741–2743 (2014).
- [54] Heinz, T., Chen, C., Ricard, D., Shen, Y., “Spectroscopy of Molecular Monolayers by Resonant Second-Harmonic Generation,” *Phys. Rev. Lett.* **48**(7), 478–481 (1982).
- [55] Huang, W., Helvenston, M., Casson, J. L., Wang, R., Bardeau, J.-F., Lee, Y., Johal, M. S., Swanson, B. I., Robinson, J. M., et al., “Synthesis, Characterization, and NLO Properties of a Phenothiazine–Stilbazole Monolayer,” *Langmuir* **15**(19), 6510–6514 (1999).
- [56] Roscoe, S. B., Kakkar, A. K., Marks, T. J., Malik, A., Durbin, M. K., Lin, W., Wong, G. K., Dutta, P., “Self-Assembled Chromophoric NLO-Active Monolayers. X-ray Reflectivity and Second-Harmonic Generation as Complementary Probes of Building Block–Film Microstructure Relationships,” *Langmuir* **12**(17), 4218–4223 (1996).
- [57] Facchetti, A., van der Boom, M. E., Abbotto, A., Beverina, L., Marks, T. J., Pagani, G. A., “Design and Preparation of Zwitterionic Organic Thin Films: Self-Assembled Siloxane-Based, Thiophene-Spaced N -Benzylpyridinium Dicyanomethanides as Nonlinear Optical Materials,” *Langmuir* **17**(19), 5939–5942 (2001).
- [58] Facchetti, A., Abbotto, A., Beverina, L., van der Boom, M. E., Dutta, P., Evmenenko, G., Marks, T. J., Pagani, G. A., “Azinium–( $\pi$ -Bridge)–Pyrrole NLO-Phores: Influence of

- Heterocycle Acceptors on Chromophoric and Self-Assembled Thin-Film Properties #,” *Chem. Mater.* **14**(12), 4996–5005 (2002).
- [59] Facchetti, A., Abbotto, A., Beverina, L., Boom, M. E. Van Der., Dutta, P., Evmenenko, G., Pagani, G. A., Marks, T. J., “Layer-by-Layer Self-Assembled Pyrrole-Based Donor-Acceptor Chromophores as Electro-Optic Materials,” *Chem. Mater.* **15**, 1064–1072 (2003).
- [60] Clays, K., Hendrickx, E., Triest, M., Persoons, A., “Second-order nonlinear optics in isotropic liquids : Hyper-Rayleigh scattering in solution.,” *J. Mol. Liq.* **67**(1995), 133–155 (1995).
- [61] Van Cleuvenbergen, S., Asselberghs, I., García-Frutos, E. M., Gómez-Lor, B., Clays, K., Pérez-Moreno, J., “Dispersion Overwhelms Charge Transfer in Determining the Magnitude of the First Hyperpolarizability in Triindole Octupoles,” *J. Phys. Chem. C* **116**(22), 12312–12321 (2012).
- [62] Olbrechts, G., Strobbe, R., Clays, K., Persoons, A., “High-frequency demodulation of multi-photon fluorescence in hyper-Rayleigh scattering,” *Rev. Sci. Instrum.* **69**(6), 2233 (1998).
- [63] Olbrechts, G., Clays, K., Wostyn, K., Persoons, A., “Fluorescence-free hyperpolarizability values by near-infrared, femtosecond hyper-Rayleigh scattering,” *Synth. Met.* **115**(1-3), 207–211 (2000).